Supplementary Materials

The effects of particle-induced oxidative damage from exposure to airborne fine particulate matter components in the vicinity of landfill sites on Hong Kong

K. H. Lui[1,10], Tim P. Jones[2], Kelly BéruBé[3], Steven Sai Hang Ho[4], S.H.L.Yim[5,6], Jun-Ji Cao[4,7], S. C. Lee[8], Linwei Tian[9], Dae Wi Min[10], K. F. Ho[1*]

[1] *The Jockey Club School of Public Health and Primary Care, The Chinese University of Hong Kong, Hong Kong, China*

[2] *School of Earth and Ocean Sciences, Cardiff University, Park Place, Cardiff, U.K.*

[3] *School of Biosciences, Cardiff University, Museum Avenue, Cardiff, U.K.*

[4] *Key Division of Atmospheric Sciences, Desert Research Institute, Reno, NV 89512, U.S.A.*

[5] *Department of Geography and Resource Management, The Chinese University of Hong Kong, Hong Kong, China*

[6] *Stanley Ho Big Data Decision Analytics Research Centre, The Chinese University of Hong Kong, Shatin, N.T., Hong Kong, China*

[7] *Institute of Global Environmental Change, Xi'an Jiaotong University, Xi'an, China*

[8] *Department of Civil and Structural Engineering, Research Center of Urban Environmental Technology and Management, The Hong Kong Polytechnic University, Hong Kong, China*

[9] *School of Public Health, The University of Hong Kong, Hong Kong, China*

[10] *Division of Environmental Science and Engineering, Pohang University of Science and Technology (POSTECH), Pohang 37673, Korea*

[*]Corresponding author. Tel.: +852 22528763; fax: +852 26063500

E-mail address: kfho@cuhk.edu.hk

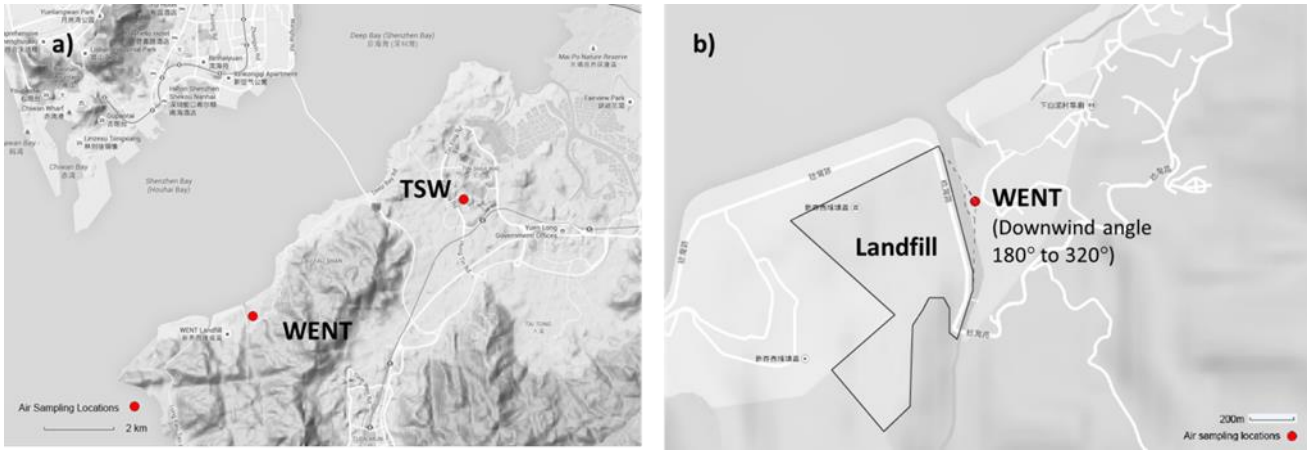

Figure S1 Sampling location of a) WENT Background Site at Tin Shui Wai and b) WENT Site at Ha Pak Nai.

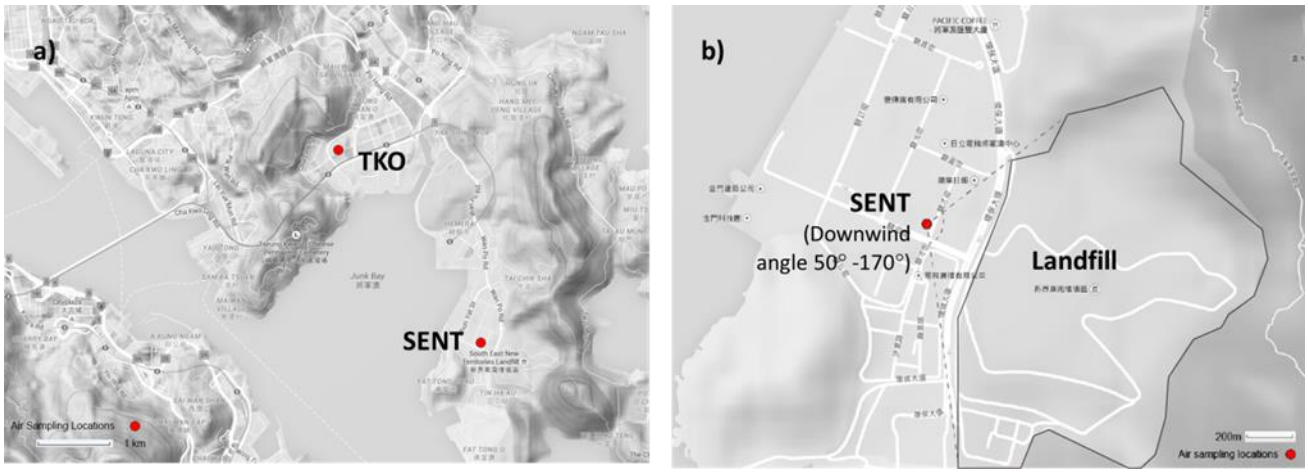

Figure S2 Sampling location of a) SENT Background Site at Tseung Kwan O and b) SENT Site.

Figure S3 URG $PM_{2.5}$ filter-based sampler at WENT sampling location.

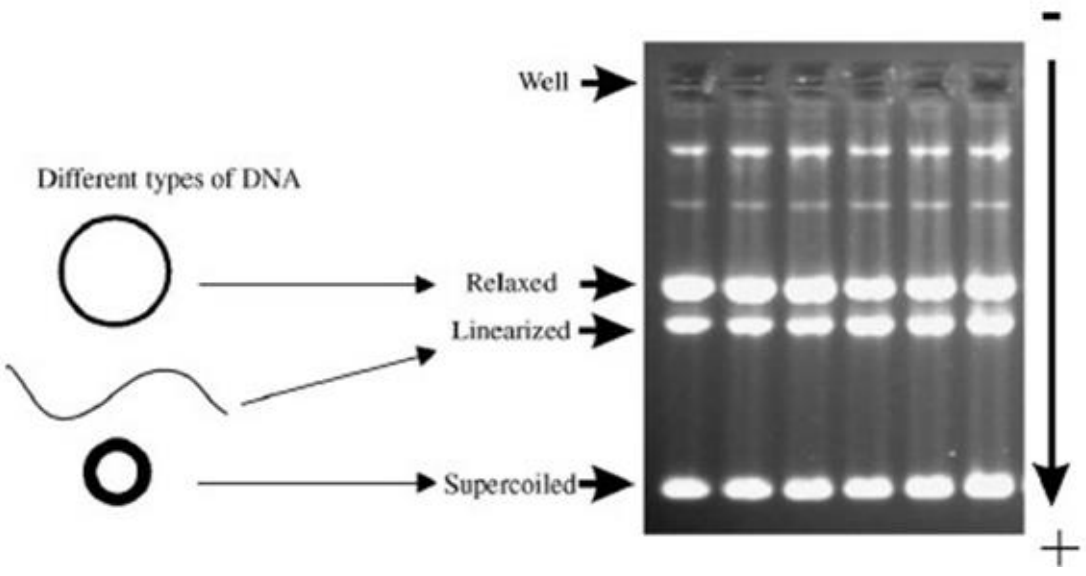

Figure S4 Identification of different types of plasmid ΦX174-RF DNA (Promega, London, UK) in gel electrophoresis.

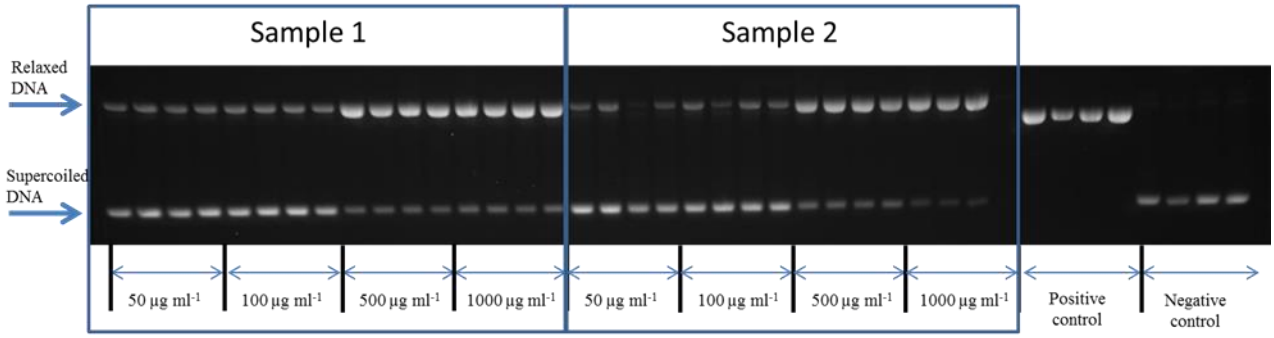

Figure S5 Gel images demonstrate oxidative damage to supercoiled DNA induced by $PM_{2.5}$ sample.

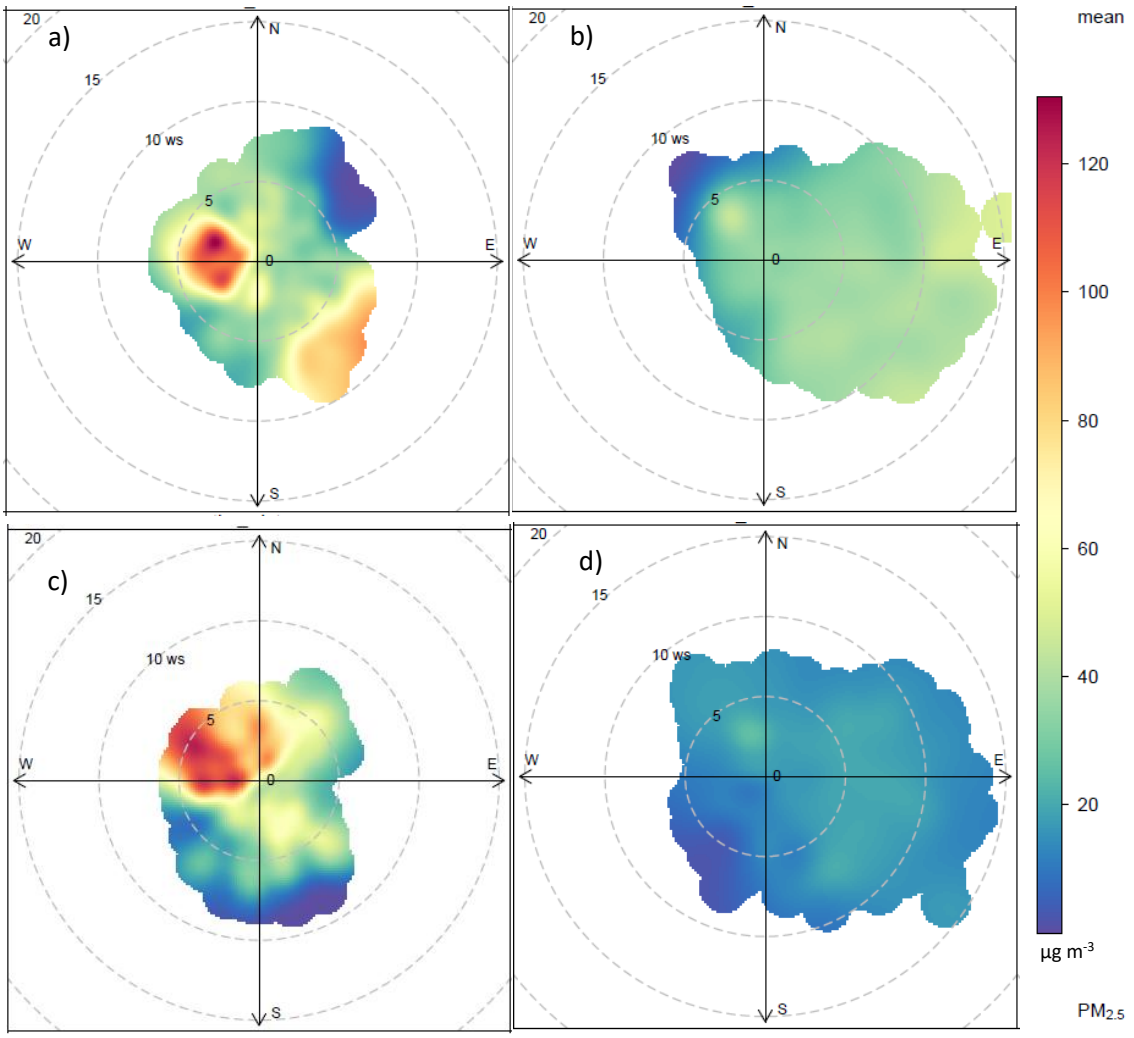

96

97 Figure S6 Pollution roses of $PM_{2.5}$ concentrations (µg m^3) in winter and summer at (a and

98 c) WENT and (b and d) SENT site. The unit of wind speed is m/s.

99

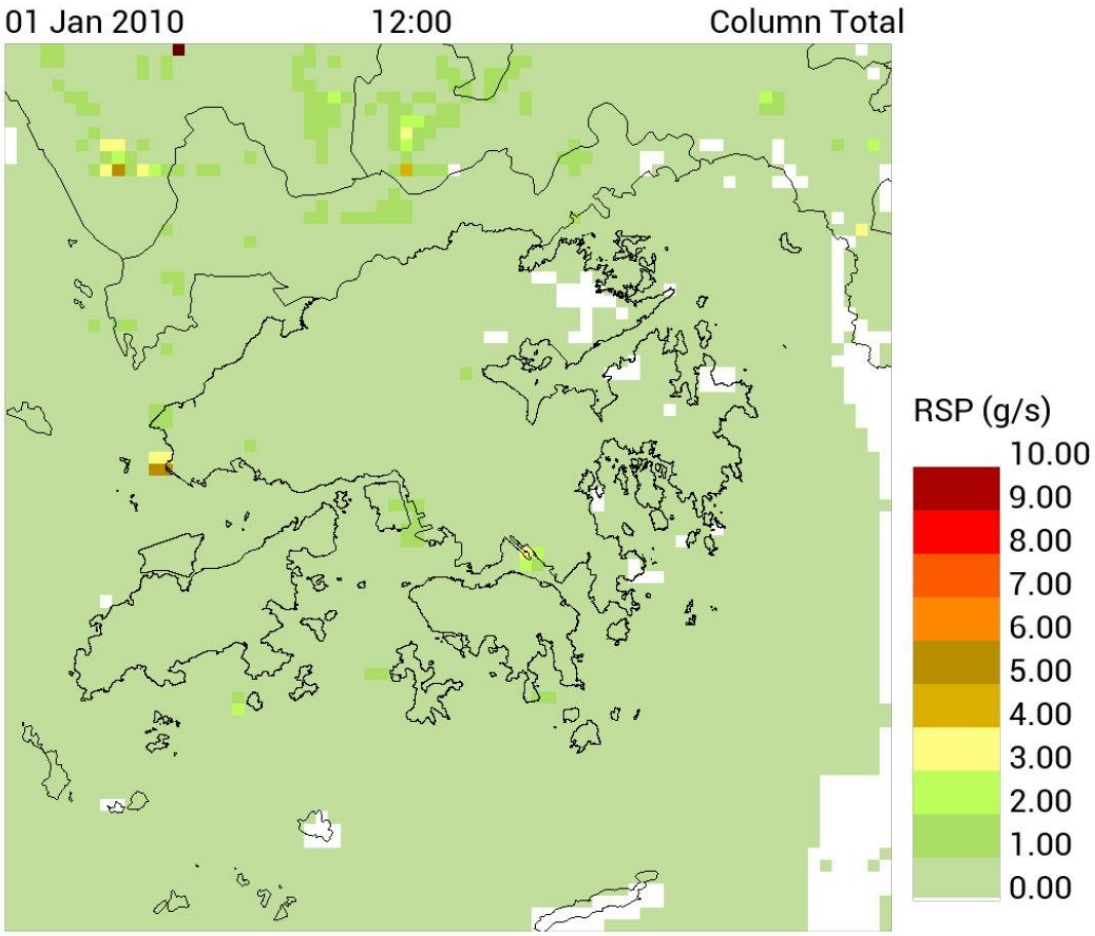

Figure S7 A map of respirable suspended particulate (RSP) emissions (g/s) over Hong Kong. Source: The Hong Kong Environmental Protection Department, The Government of the Hong Kong Special Administrative Region. Available at: https://www.epd.gov.hk/epd/sites/default/files/epd/english/environmentinhk/air/guide_ref/files/RSP.jpg

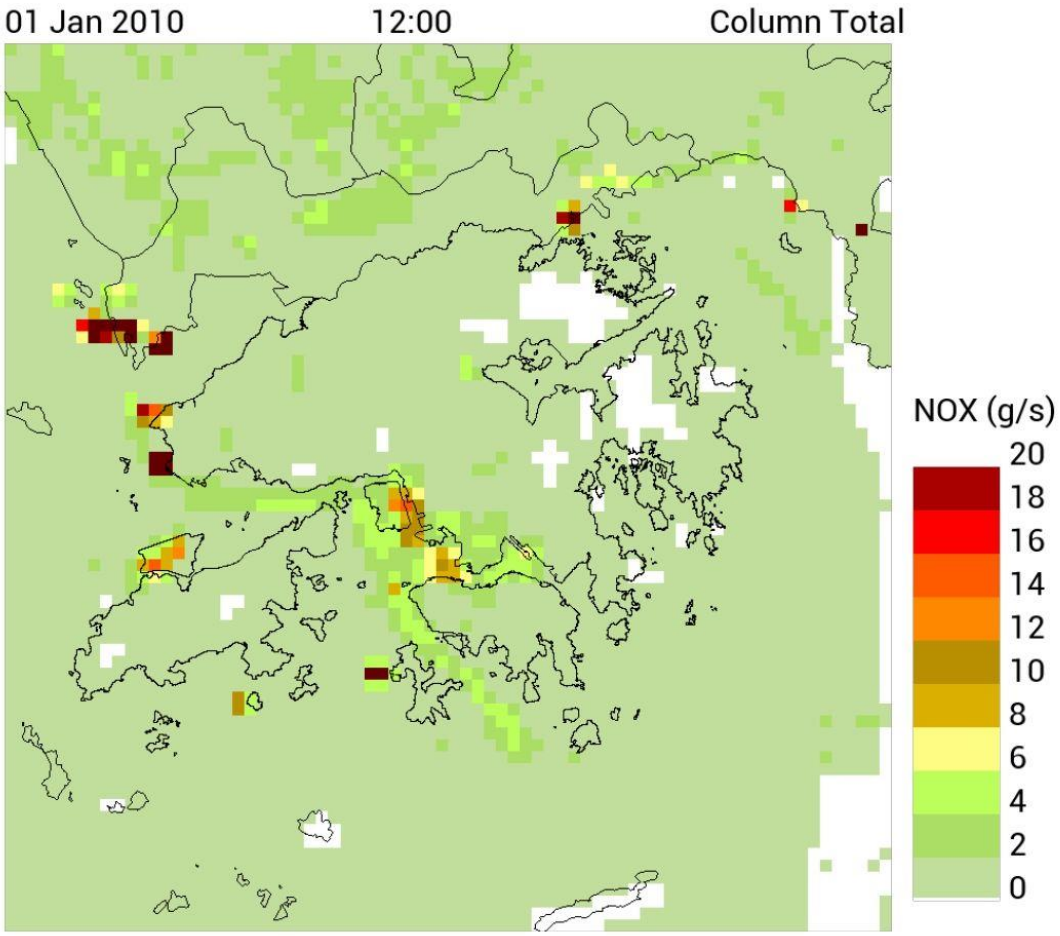

Figure S8 A map of nitrogen oxides (NO_x) emissions (g/s) over Hong Kong. Source: The Hong Kong Environmental Protection Department, The Government of the Hong Kong Special Administrative Region. Available at: https://www.epd.gov.hk/epd/sites/default/files/epd/english/environmentinhk/air/guide_ref/files/NOx.jpg

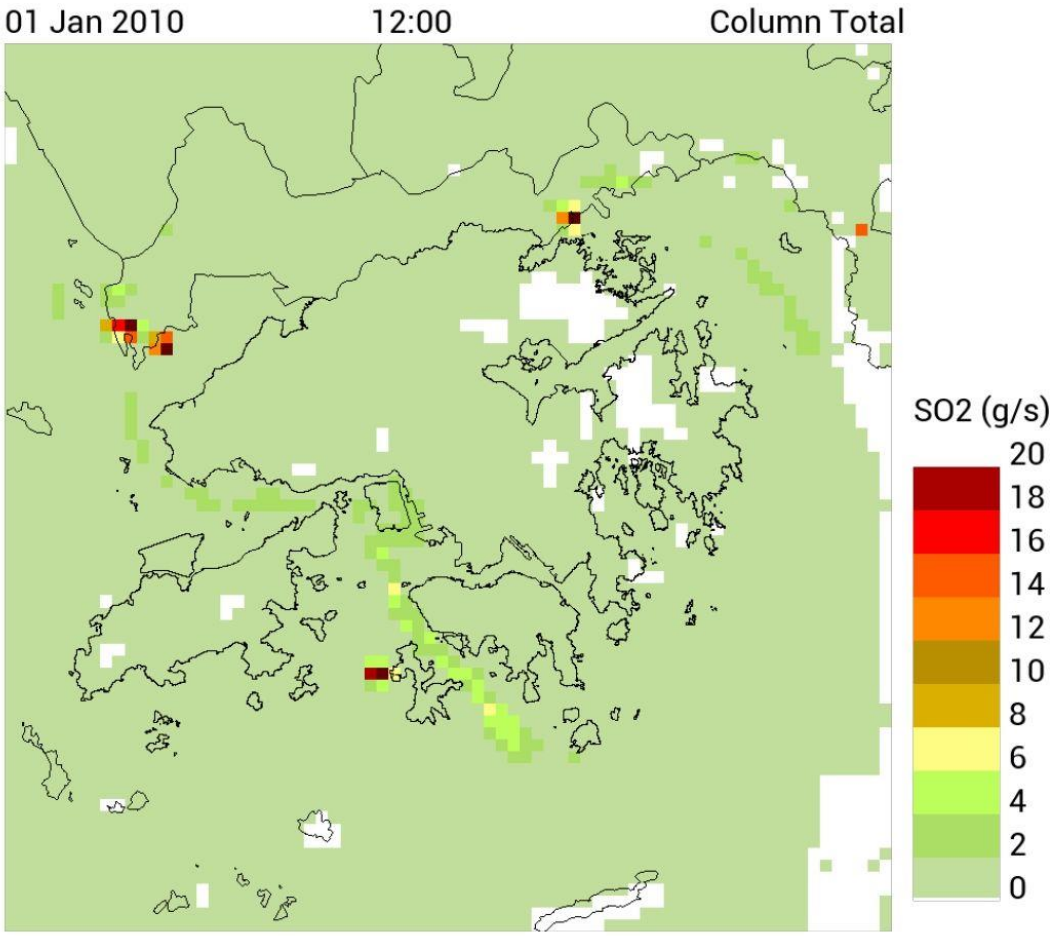

Figure S9 A map of sulfur dioxide (SO_2) emissions (g/s) over Hong Kong. Source: The Hong Kong Environmental Protection Department, The Government of the Hong Kong Special Administrative Region. Available at: https://www.epd.gov.hk/epd/sites/default/files/epd/english/environmentinhk/air/guide_ref/files/SO2.jpg

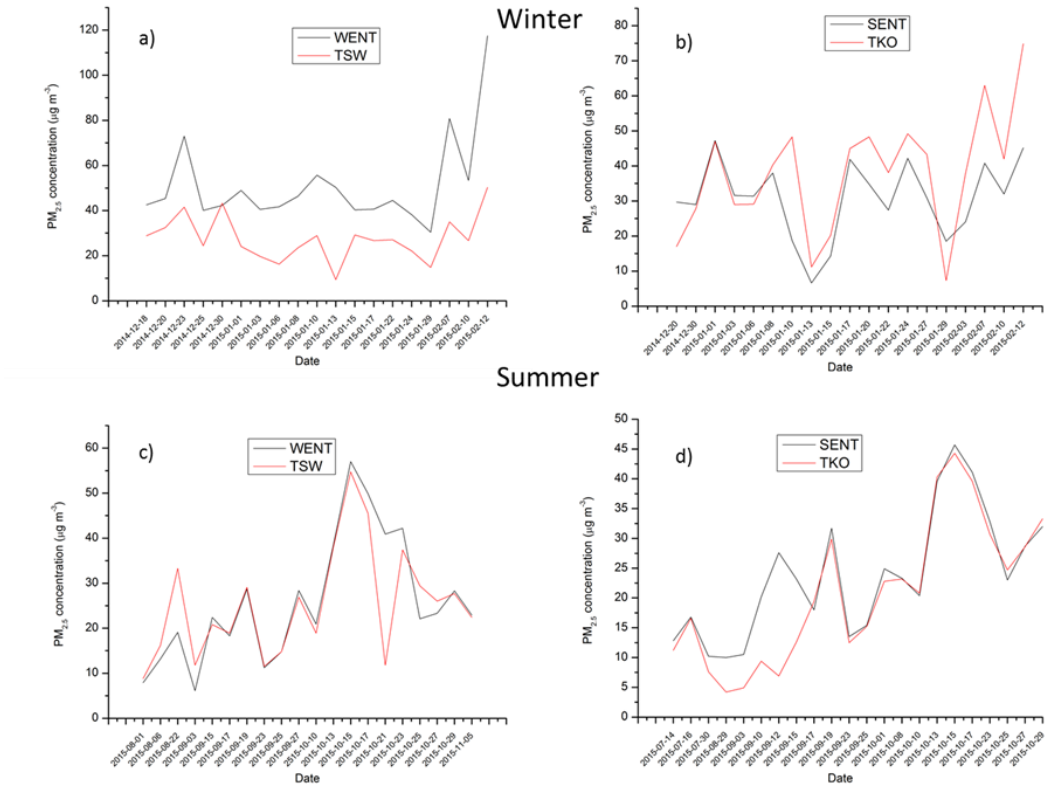

Figure S10 Daily variations of $PM_{2.5}$ between: WENT and TSW in winter (a) and summer (c) ; between SENT and TKO in winter (b) and summer (d).

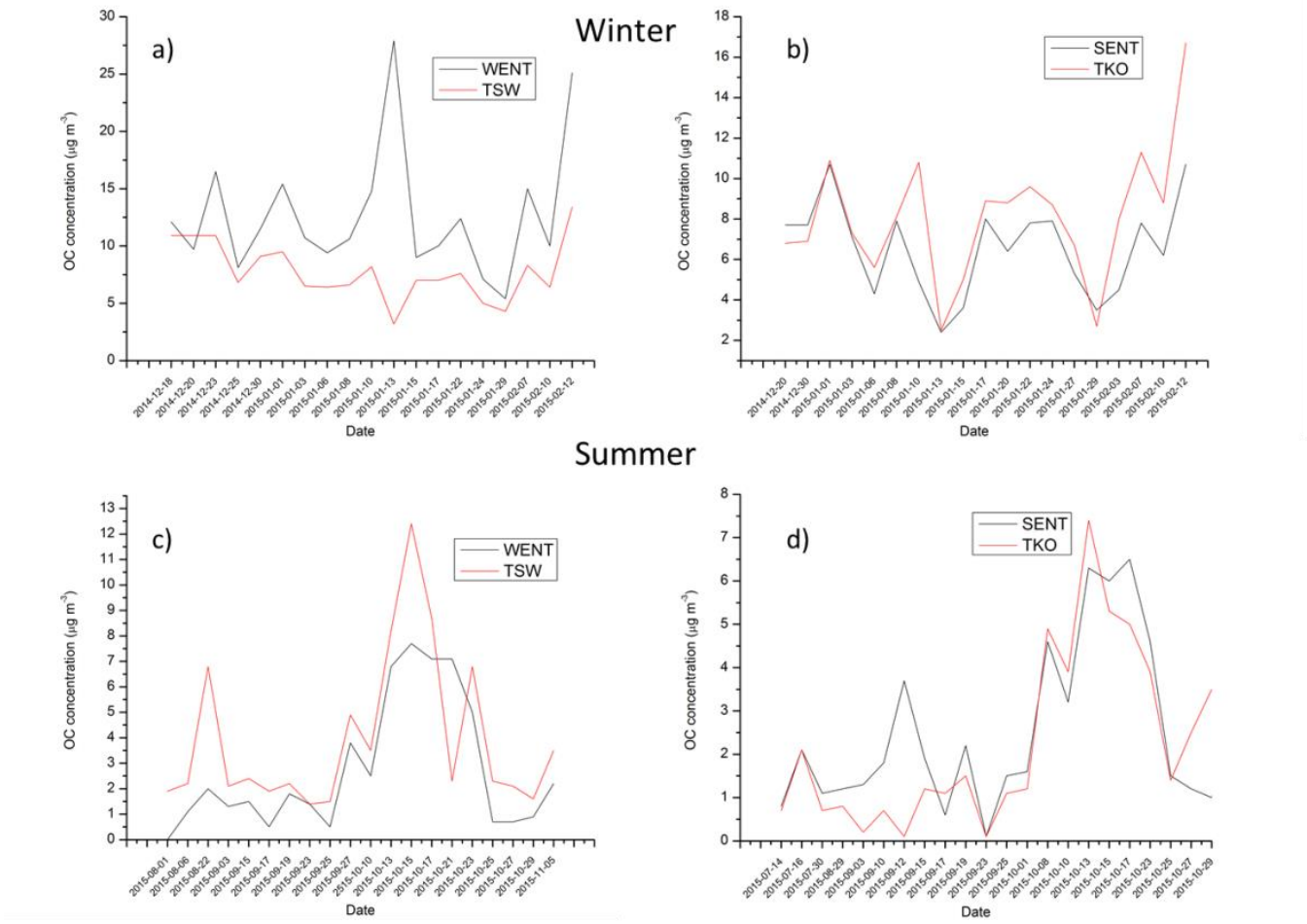

130

131 Figure S11 Daily variation of OC concentrations between: WENT and TSW in winter (a)

132 and summer (c); between SENT and TKO in winter (b) and summer (d).

133

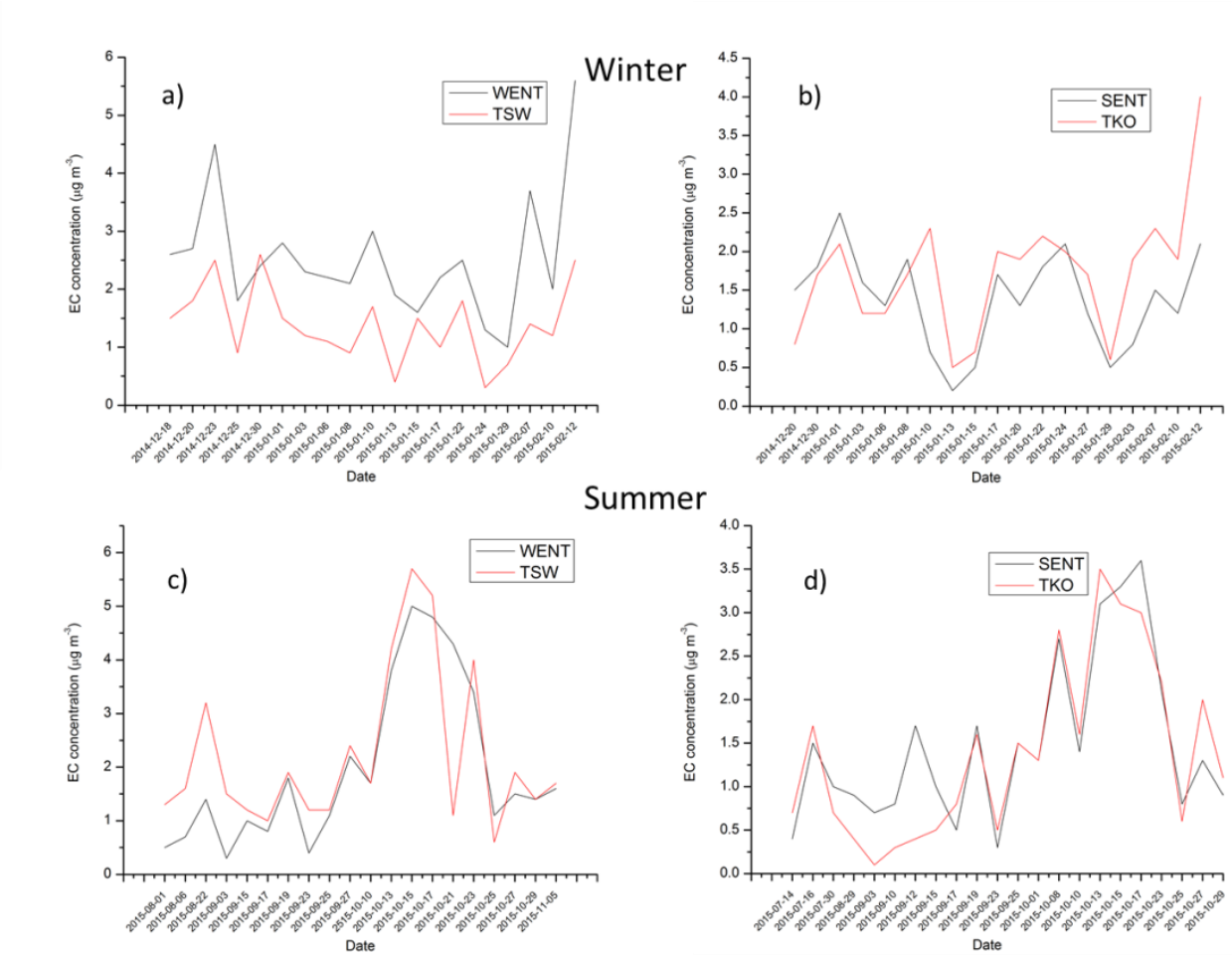

Figure S12 Daily variation of EC concentrations between: WENT and TSW in winter (a) and summer (c); between SENT and TKO in winter (b) and summer (d).

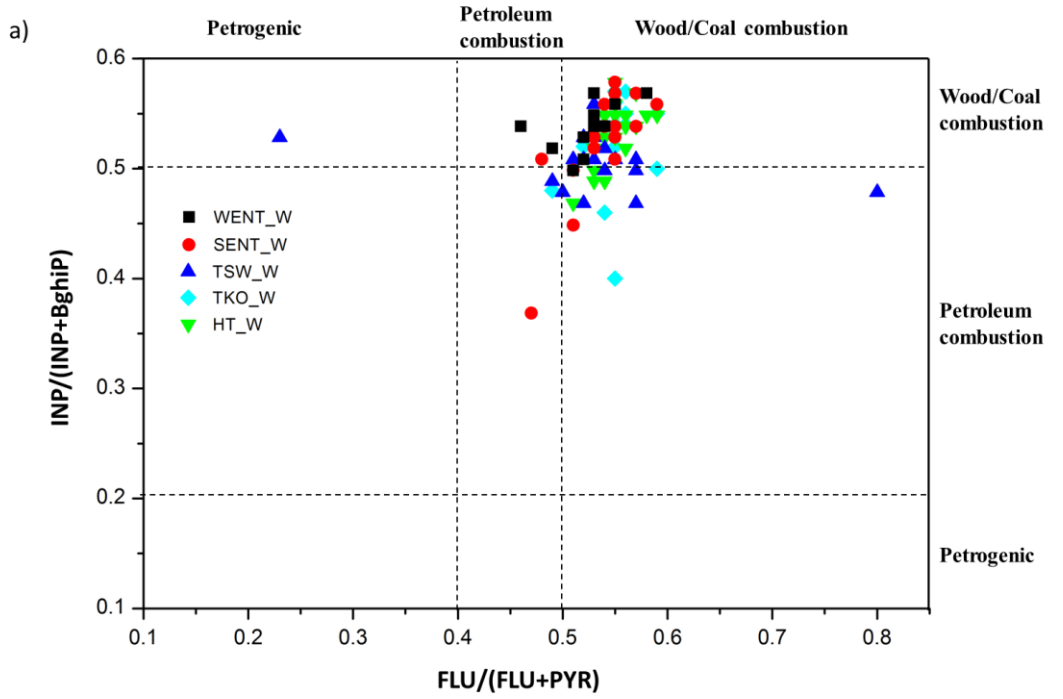

138

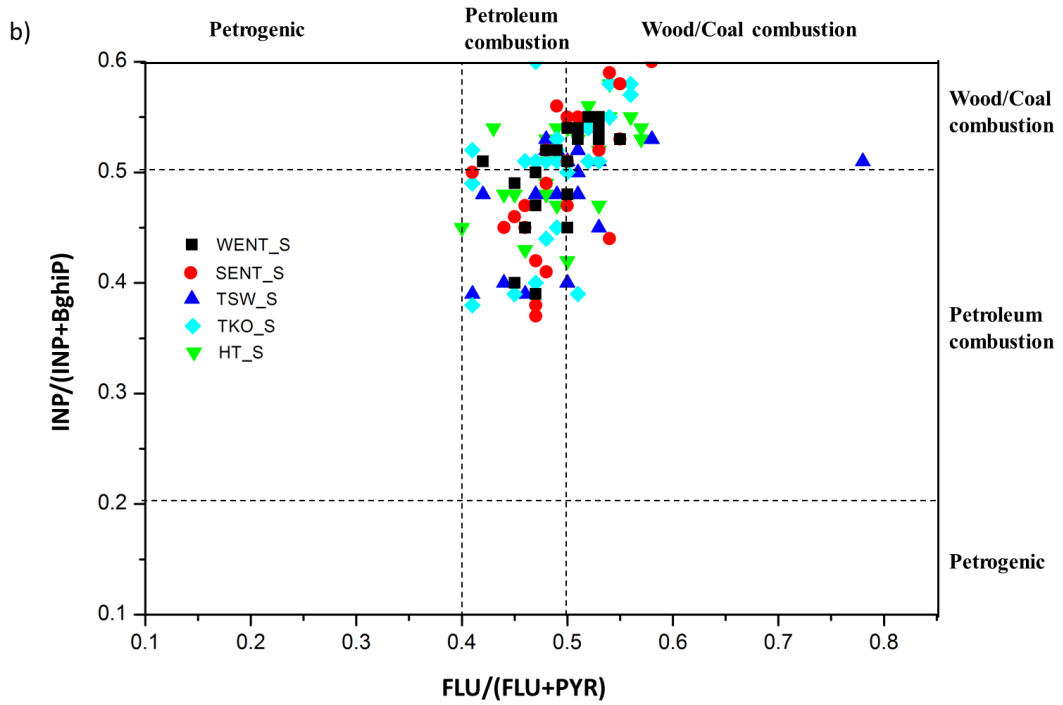

139

140 Figure S13 Correlations between PAHs diagnostic ratios FLU/(FLU+PYR) and

141 INP/(INP+BghiP) at five sampling locations in winter (a) and summer (b).

142

143 Table S1 Average meteorological parameter during the sampling period

144

		Total Rainfall (mm)
WENT	Winter	12.4±10.7
	Summer	131.4±78.8
SENT	Winter	35.8±7.7
	Summer	182.7±136.9
HT	Winter	28.0±3.2
	Summer	162.6±158.9

145

146 Table S2 The analyzed chemical components in this study.

Name	Abb*	Name	Abb	Name	Abb
Metal		***Water-soluble ions***			
Magnesium	Mg	Sodium ion	Na^+	Chrysene	CHR
Calcium	Ca	Potassium ion	K^+	Benzo[*b*]fluoranthene	BbF
Vanadium	V	Ammonium	NH_4^+	Benzo[*k*]fluoranthene	BkF
Chromium	Cr	Sulphate	SO_4^{2-}	Benzo[*a*]fluoranthene	BaF
Manganese	Mn	Nitrate	NO_3^-	Benzo[*e*]pyrene	BeP
Iron	Fe	Chloride	Cl^-	Benzo[*a*]pyrene	BaP
Nickel	Ni	***PAHs***		Perylene	PER
Copper	Cu	Acenaphthene	ACE	Indeno[*1,2,3-cd*]pyrene	INP
Zinc	Zn	Fluorene	FLU	dibenz[*a,h*]anthracene	DahA
Arsenic	As	Phenanthrene	PHE	Benzo[*ghi*]perylene	BghiP
Cadmium	Cd	Anthracene	ANT	Coronene	COR
Barium	Ba	Fluoranthene	FLT	***Carbonaceous species***	

Lead	Pb	Pyrene	PYR	Organic carbon	OC
		Benz[*a*]anthracene	BaA	Elemental carbon	EC

147 *Abb = abbreviation

148

149 Table S3 The average concentration of $PM_{2.5}$ in five sampling locations during winter and

150 summer.

Concentration ($\mu g\ m^{-3}$)	Winter		Summer	
Sampling location	N**	mean (std)*	N	mean (std)
WENT	19	51.2 (20.0)	20	25.8 (13.8)
SENT	19	30.8 (10.8)	24	24.1 (10.0)
TSW	19	27.6 (10.0)	20	25.2 (12.2)
TKO	19	37.8 (17.0)	24	21.5 (11.7)
HT	22	41.5 (14.6)	28	22.7 (11.4)

151 *std = standard deviation

152 **N = number of sampling days

153

154 Table S4 The average concentration of OC and EC in five sampling locations during

155 winter and summer.

Concentration ($\mu g\ m^{-3}$)	Winter mean (std)*		Summer mean (std)	
Sampling location	OC	EC	OC	EC
WENT	12.7 (5.7)	2.5 (1.1)	2.7(2.6)	1.9 (1.5)
SENT	6.6 (2.3)	1.4 (0.6)	2.6 (1.9)	1.5 (0.9)

TSW	7.8 (2.5)	1.4 (0.7)	3.9 (3.1)	2.2 (1.5)
TKO	8.1 (3.2)	1.7 (0.8)	2.4 (2.0)	1.4 (1.0)
HT	7.3 (3.5)	2.1 (0.8)	1.8 (1.8)	1.0 (0.8)

*std = standard deviation

Table S5 The average concentration of water-soluble inorganic ions in five sampling locations during winter and summer.

Components	Concentration ($\mu g\ m^{-3}$)	WENT mean (std)*	SENT mean (std)	TSW mean (std)	TKO mean (std)	HT mean (std)
Cl^-	Winter	0.50 (0.40)	0.31 (0.22)	0.22 (0.24)	0.36 (0.30)	1.11 (1.01)
	Summer	0.48 (0.34)	0.43 (0.12)	0.43 (0.07)	0.55 (0.33)	0.47 (0.26)
NO_3^-	Winter	8.23 (5.65)	3.93 (1.90)	4.07 (2.20)	4.37 (2.58)	3.83 (2.34)
	Summer	2.25 (1.46)	2.25 (0.89)	2.22 (0.95)	1.85 (0.86)	1.68 (0.86)
SO_4^{2-}	Winter	12.43 (5.20)	10.44 (3.83)	7.23 (2.38)	12.96 (5.71)	12.32 (4.87)
	Summer	9.23 (3.68)	9.43 (4.23)	9.47 (3.62)	8.73 (4.61)	9.38 (4.16)
Na^+	Winter	0.86 (0.25)	1.16 (0.66)	0.42 (0.22)	1.18 (0.41)	1.62 (0.69)
	Summer	1.58 (0.30)	1.42 (0.28)	1.55 (0.25)	1.50 (0.32)	1.91 (0.67)
NH_4^+	Winter	5.69 (3.21)	4.17 (1.33)	3.14 (1.29)	5.06 (2.56)	4.28 (2.18)
	Summer	1.81 (1.38)	1.61 (1.16)	1.89 (1.31)	1.57 (1.26)	1.33 (1.03)
K^+	Winter	1.06 (0.45)	0.56 (0.25)	0.58 (0.25)	0.76 (0.39)	0.76 (0.43)
	Summer	0.09 (0.13)	0.06 (0.13)	0.06 (0.10)	0.05 (0.10)	0.06 (0.11)
Total	Winter	28.77 (13.81)	20.35 (7.78)	15.66 (5.51)	24.69 (11.21)	23.92 (9.61)
	Summer	15.44 (6.36)	15.21 (6.11)	15.62 (5.67)	13.65 (7.16)	14.77 (6.18)

*std = standard deviation

Table S6 The average concentration of inorganic elements in five sampling locations during winter and summer.

Components	Concentration ($\mu g\ m^{-3}$)	WENT mean (std)*	SENT mean (std)	TSW mean (std)	TKO mean (std)	HT mean (std)
Mg	Winter	100.2 (26.2)	95.6 (50.1)	76.4 (25.6)	92.2 (39.6)	133.6 (55.7)
	Summer	35.4 (15.8)	39.8 (18.4)	46.3 (21.2)	44.9 (14.6)	67.1 (30.2)
Ca	Winter	489.9 (172.3)	842.8 (732.4)	765.6 (193.3)	487.5 (376.2)	819.2 (190.2)
	Summer	335.7 (142.4)	265.2 (153.8)	455.4 (166.0)	209.7 (153.7)	347.8 (142.9)
V	Winter	10.5 (9.3)	6.0 (6.9)	5.9 (5.0)	6.2 (6.4)	8.6 (10.4)
	Summer	15.6 (8.8)	16.7 (7.7)	14.1 (8.8)	16.2 (10.1)	22.0 (11.2)
Cr	Winter	11.5 (8.9)	7.6 (3.8)	16.7 (13.6)	9.5 (6.8)	22.0 (16.4)
	Summer	7.0 (3.6)	9.1 (9.8)	15.1 (17.6)	6.9 (8.0)	9.0 (9.4)
Mn	Winter	22.5 (6.8)	10.3 (4.5)	12.4 (6.2)	15.1 (5.7)	10.4 (6.2)
	Summer	13.1 (7.8)	13.7 (8.9)	15.6 (13.3)	16.0 (16.8)	9.7 (5.8)
Fe	Winter	582.8 (142.3)	432.2 (141.6)	473.4 (167.2)	542.5 (192.7)	288.4 (139.7)
	Summer	124.3 (71.3)	144.6 (76.2)	123.4 (79.5)	165.0 (136.5)	83.8 (75.2)
Ni	Winter	16.8 (9.9)	22.7 (59.2)	32.2 (44.2)	28.7 (47.5)	31.6 (26.6)
	Summer	23.4 (22.8)	23.9 (17.4)	34.4 (42.6)	22.7 (27.0)	24.8 (20.3)
Cu	Winter	28.8 (16.4)	18.2 (16.3)	27.1 (25.6)	26.8 (18.1)	37.8 (32.1)
	Summer	23.7 (25.1)	21.4 (23.1)	40.5 (79.7)	24.9 (27.4)	15.9 (16.9)
Zn	Winter	168.4 (60.6)	116.2 (50.0)	85.5 (43.4)	128.5 (56.8)	150.3 (67.1)
	Summer	88.5 (72.4)	84.0 (74.2)	85.3 (72.7)	105.1 (164.5)	77.8 (80.6)
As	Winter	8.1 (4.1)	5.2 (2.8)	4.1 (2.4)	5.8 (3.6)	5.8 (3.9)
	Summer	4.4 (3.8)	4.3 (3.9)	4.6 (4.1)	5.0 (7.0)	4.0 (3.6)
Cd	Winter	1.7 (0.8)	1.0 (0.6)	0.9 (0.5)	1.1 (0.6)	1.1 (0.7)
	Summer	0.7 (0.5)	0.5 (0.4)	0.6 (0.5)	0.7 (1.1)	0.5 (0.4)
Ba	Winter	6.9 (5.5)	4.4 (2.4)	5.0 (2.7)	5.5 (2.2)	4.3 (3.8)
	Summer	20.8 (23.6)	22.4 (24.5)	22.7 (24.4)	20.1 (21.9)	16.0 (22.7)
Pb	Winter	53.5 (22.0)	33.3 (17.6)	29.3 (17.1)	38.7 (20.6)	39.7 (21.5)
	Summer	23.0 (16.1)	17.2 (12.9)	23.4 (17.4)	17.3 (15.1)	16.8 (13.5)

164 *std = standard deviation

165

166 Table S7 The average concentrations of PAHs in five sampling locations during winter

167 and summer.

Components	Concentration ($ng\ m^{-3}$)	WENT		SENT		TSW		TKO		HT	
		mean	std*	mean	std	mean	std	mean	std	mean	std
ACE	Winter	0.43	0.32	0.10	0.04	0.29	0.36	0.27	0.15	0.18	0.15
	Summer	0.03	0.01	0.02	0.01	0.03	0.02	0.03	0.01	0.02	0.01
FLU	Winter	0.30	0.24	0.05	0.05	0.10	0.15	0.19	0.16	0.09	0.05
	Summer	0.05	0.02	0.05	0.01	0.06	0.03	0.05	0.02	0.05	0.04
PHE	Winter	1.01	0.78	0.41	0.24	0.57	0.39	0.70	0.43	0.57	0.27
	Summer	0.17	0.06	0.17	0.05	0.21	0.07	0.19	0.06	0.14	0.07
ANT	Winter	0.15	0.11	0.04	0.02	0.08	0.04	0.08	0.06	0.05	0.02
	Summer	0.05	0.02	0.04	0.01	0.05	0.02	0.04	0.01	0.04	0.02
FLT	Winter	1.25	0.96	0.62	0.40	0.72	0.37	0.79	0.34	0.80	0.47

	Summer	0.14	0.10	0.14	0.10	0.16	0.10	0.16	0.11	0.10	0.08
PYR	Winter	1.14	0.88	0.51	0.32	0.59	0.21	0.64	0.26	0.64	0.37
	Summer	0.14	0.09	0.14	0.08	0.16	0.10	0.15	0.09	0.10	0.07
BaA	Winter	0.49	0.46	0.18	0.13	0.24	0.13	0.22	0.09	0.20	0.10
	Summer	0.05	0.04	0.03	0.02	0.05	0.04	0.04	0.03	0.02	0.02
CHR	Winter	1.23	1.13	0.39	0.21	0.55	0.27	0.49	0.19	0.47	0.26
	Summer	0.11	0.08	0.10	0.07	0.15	0.08	0.12	0.08	0.07	0.06
BbF	Winter	1.23	0.83	0.43	0.26	0.74	0.49	0.52	0.19	0.53	0.30
	Summer	0.15	0.11	0.11	0.10	0.19	0.13	0.14	0.11	0.09	0.08
BkF	Winter	0.90	0.65	0.28	0.16	0.56	0.39	0.40	0.14	0.37	0.19
	Summer	0.12	0.09	0.08	0.08	0.15	0.11	0.10	0.08	0.07	0.06
BaF	Winter	0.17	0.13	0.05	0.02	0.10	0.07	0.07	0.02	0.06	0.03
	Summer	0.02	0.02	0.01	0.01	0.03	0.02	0.02	0.01	0.01	0.01

BeP	Winter	0.77	0.54	0.25	0.14	0.49	0.34	0.32	0.10	0.32	0.17
	Summer	0.11	0.08	0.07	0.06	0.14	0.09	0.09	0.07	0.06	0.05
BaP	Winter	0.55	0.42	0.19	0.12	0.34	0.22	0.23	0.09	0.23	0.14
	Summer	0.09	0.08	0.06	0.06	0.11	0.09	0.07	0.06	0.05	0.05
PER	Winter	0.10	0.08	0.03	0.02	0.06	0.04	0.05	0.02	0.16	0.38
	Summer	0.06	0.13	0.02	0.01	0.03	0.03	0.02	0.02	0.01	0.01
INP	Winter	0.87	0.64	0.27	0.16	0.58	0.48	0.34	0.12	0.37	0.22
	Summer	0.12	0.11	0.07	0.09	0.14	0.12	0.08	0.09	0.07	0.07
BghiP	Winter	0.76	0.58	0.24	0.13	0.58	0.52	0.31	0.10	0.32	0.19
	Summer	0.11	0.10	0.06	0.07	0.14	0.11	0.08	0.08	0.06	0.06
DahA	Winter	0.13	0.07	0.04	0.03	0.07	0.05	0.05	0.03	0.04	0.03
	Summer	0.02	0.01	0.01	0.01	0.02	0.02	0.01	0.01	0.01	0.01
COR	Winter	0.18	0.14	0.05	0.04	0.13	0.14	0.06	0.03	0.07	0.05

	Summer	0.04	0.04	0.03	0.03	0.04	0.04	0.03	0.03	0.02	0.02
Total	Winter	11.63	8.04	4.02	2.29	6.79	4.05	5.74	1.97	5.43	2.80
	Summer	1.58	0.99	1.20	0.76	1.87	1.12	1.41	0.82	1.00	0.66

*std = standard deviation

Table S8 Correlations between wind flow from landfills and $PM_{2.5}$ components.

	WENT		SENT	
Components	Winter	Summer	Winter	Summer
$PM_{2.5}$				
Mg				
Ca				
V	++**	++	++	
Cr				
Mn				
Fe				
Ni				
Cu	++		++	
Zn				
As				
Cd				
Sb				
Ba				
Pb				
OC				
EC				
Cl^-	++		++	
NO_3^-	+*		+	

SO_4^{2-}				
Na^+	+		+	+
NH_4^+				
K^+		+		
Total PAHs				

*+, positive correlation, $p < 0.05$.
**++, positive correlation, $p < 0.01$.

Text S1 Sample and meteorological parameter collection

The $PM_{2.5}$ samples were collected simultaneously on 47-mm Teflon (Pall Life Sciences, Ann Arbor, MI) and 47-mm quartz-fibre filters (Whatman Inc., Clifton, NJ) at all sites with URG $PM_{2.5}$ samplers (URG-2000-30EH) as shown in Figure S3 (Supplementary Material). WindSonic sensor (Gill Instruments, Model 1405) and real-time $PM_{2.5}$ monitors (MetONE, Met One Instruments, Model ES-642) were installed at two locations in proximity to the landfill sites in order to determine diurnal variations of particulate level, wind speed and direction. The real-time $PM_{2.5}$ monitor is a type of nephelometer which automatically quantifies real-time $PM_{2.5}$ concentration levels using the principle of forward laser light scatter. This scattered light is collected onto a photodiode detector at near-forward angle, and the resulting electronic signal is converted to continuous, real-time measurement of airborne particulate mass concentrations. The resolution of $PM_{2.5}$ data collection was set at 4 seconds to synchronize with the time resolution of the WindSonic sensor for meteorological data collection.

Twenty-four hours integrated $PM_{2.5}$ samples were collected in winter (December to March, 2014-15) and summer (July to November, 2015) in every 3 days intervals. A total of 214 filter samples were collected for this study. A microbalance (Sartorius Model MC5 Microbalance, Göttingen) with 1 µg precision was used for the mass concentration measurements. Filter preparation and gravimetric analysis were conducted in a high-efficiency particulate absorption (HEPA) clean room that satisfied ISO 14644 (Class 7) at The Hong Kong Polytechnic

University in Hong Kong. Microbalance and working mass standards were calibrated by an external contractor on a yearly basis. Temperature (T), relative humidity (RH) and working mass standards verification was calibrated in every quarter of the year. The balance was calibrated with 200 and 100 Class 1 standard weights and tare was set before weighing each batch of filters. After weighing every 10 filters, 200 and 100 mg calibration and tare were re-applied in the process. All initial filters weighing procedures were carried out 30 days before the sampling period. Post-sampling weighing procedures were carried out no later than 30 days after the end of sampling period. All filters were stored at -20 °C and in dark prior to the analysis. The meteorological parameter was collected by the Hong Kong Observatory (HKO) climatological database.

Text S2 Inductively coupled plasma mass spectroscopy (ICP-MS) for elements analysis

Total metal concentrations were analysed using inductively coupled plasma mass spectrometry (ICP-MS) (Perkin Elmer Sciex ELAN 6100 DRC^{plus}) (Jones et al., 2006). The sample was prepared by digesting half of a filter using concentrated nitric acid (Primar grade, Fisher). The sample solution was then heated progressively to 200°C in a heating block for 2 hr. The solution was diluted with Milli-Q water to 10 ml for the ICP-MS analysis. The detection limits were in a range of 0.1-1 ppt. The analysed elements are shown in Table S2 (Supplementary Material).

Text S3 Ion chromatography (IC) for water-soluble inorganic ions analysis

One quarter of quartz filter was extracted with 10 mL of distilled deionized water and the extractant was used for ion chromatographic (IC) (Dionex DX-600) analysis. IonPac CS12A

and AS14A columns were used for the separation of cations and anions, respectively. Six species were analysed and the detection limits for Na^+, NH_4^+, K^+, SO_4^{2-}, NO_3^-, and Cl^- were 4.6, 4.0, 10.0, 0.5, 15.0 and 20.0 ppb, respectively. Details of the chemical analysis can be referred to Zhang et al (Zhang et al., 2011).

Text S4 Organic carbon (OC) and elemental carbon (EC) analysis

Organic carbon (OC) and elemental carbon (EC) were analysed on a punch (0.526 cm^2) from quartz filter by thermal optical reflectance (TOR) technique following the IMPROVE_A protocol on a thermal/optical carbon analyser (DRI Model 2001, Atmoslytic Inc., Calabasas, CA). The EC and OC were all below 1.0 μg m^{-3} detection limit of the instrument. Details of the chemical analysis can be referred to Pathak et al (2011).

Text S5 Thermal desorption-gas chromatography-mass spectrometry (TD-GC/MS) for polycyclic aromatic hydrocarbons (PAHs) analysis

Concentrations of PAHs were analysed by thermally desorbing a filter strip (quartz filter) in size in the injection port of an HP 5890 gas chromatography (GC) system followed by GC separation and mass spectrometric detection. The GC was equipped with an HP-5MS (5% diphenyl / 95% dimethylsiloxane, 30 m × 0.25 mm × 0.25 μm) capillary column for the separation. The analysed PAHs are shown in Table S2 (Supplementary Material). Further

information about the TD-GC/MS method can be referred to Ho et al. (2008) and Ho et al. (2011). The detection limits were in a range of 9.2–190 pg m^{-3}.

Text S6 Plasmid scission assay (PSA) for bioreactivity analysis

The plasmid scission assay (PSA) was used to determine the capability of each sample to induce plasmid DNA damage. The level of particle–DNA interaction, and subsequent damage, was measured by the three conformations of plasmid DNA present: supercoiled (no damage), relaxed (minor damage), and linear (severe damage) as shown in Figure S4 (Supplementary Material). Due to the amount of sample required for the analysis, it was required that two filtered samples were pooled together for each bioreactivity analysis. Additional information about the procedure can be obtained from previous studies (Shao et al., 2006; Chuang et al., 2013). The particle samples were run in suspension in molecular grade water over a set range of concentrations. Twenty nanograms (20 ng) of ΦX174 RF DNA was added to the liquid and incubated. Each sample was conducted in triplicate analysis. The resultant gels were captured as images and subsequent densitometric analysis was performed with software (Genetools; Syngene system, UK). The toxic dosage of PM causing 50% DNA damage (TD_{50}) was calculated by a non-linear regression exponential rise to the maximum model.

Text S7 Details of statistical analysis

263 Mann–Whitney U test was conducted to identify seasonal variability. Kruskal-Wallis H test
264 was further used to determine the spatial variability of the analysed components. The PLS
265 regression was used to investigate relationship between physical and chemical parameters with
266 the bioreactivity response. Spearman's rank correlation coefficient analysis was performed to
267 identify the correlation between oxidative DNA damage and different chemical species.

268

269 **References**

270 Chuang, H. –C., BéruBé, K., Lung, S. –C. C., Bai, K. –J., Jones, T., 2013. Investigation into the oxidative
271 potential generated by the formation of particulate matter from incense combustion. *J. Hazard.*
272 *Mater.* 244, 142-150.
273
274 Ho, S. S. H., Yu, J. Z., Chow, J. C., Zielinska, B., Watson, J. G., Sit, E. H. L., Schauer, J. J., 2008.
275 Evaluation of an in-injection port thermal desorption-gas chromatography/mass spectrometry
276 method for analysis of non-polar organic compounds in ambient aerosol samples. *J. Chromatogr. A*
277 1200, 217-227.
278
279 Ho, S. S. H., Chow, J. C., Watson, J. G., Ng, L. P. T., Kwok, Y., Ho, K., Cao, J., 2011. Precautions for
280 in-injection port thermal desorption-gas chromatography/mass spectrometry (TD-GC/MS) as
281 applied to aerosol filter samples. *Atmos. Environ.* 45, 1491-1496.
282
283 Jones, T., Moreno, T., BéruBé, K., Richards, R., 2006. The physicochemical characterisation of
284 microscopic airborne particles in south Wales: a review of the locations and methodologies. *Sci.*
285 *Total Environ.* 360, 43-59.
286
287 Pathak, R. K., Wang, T., Ho, K., Lee, S., 2011. Characteristics of summertime PM 2.5 organic and
288 elemental carbon in four major Chinese cities: implications of high acidity for water-soluble organic
289 carbon (WSOC). *Atmos. Environ.* 45, 318-325.
290
291 Shao, L., Shi, Z., Jones, T. P., Li, J., Whittaker, A. G., Berube, K. A., 2006. Bioreactivity of particulate
292 matter in Beijing air: results from plasmid DNA assay. *Sci. Total Environ.* 367, 261-272.

293

Zhang, T., Cao, J., Tie, X., Shen, Z., Liu, S., Ding, H., Han, Y., Wang, G., Ho, K., Qiang, J., 2011. Water-soluble ions in atmospheric aerosols measured in Xi'an, China: seasonal variations and sources. *Atmos. Res.* 102, 110-119.